Production of the doubly magic nucleus ^{100}Sn in fusion and quasifission reactions via light particle and cluster emission channels

Sh. A. Kalandarov,[1,2] G. G. Adamian,[1,2] N. V. Antonenko,[1] and J. P. Wieleczko[3]
[1]*Joint Institute for Nuclear Research, 141980 Dubna, Russia*
[2]*Institute of Nuclear Physics, 702132 Tashkent, Uzbekistan*
[3]*GANIL, CEA and IN2P3-CNRS, Boîte Postale 55027, F-14076 Caen Cedex, France*
(Received 19 June 2014; published 13 August 2014)

The possibilities of production of the doubly magic nucleus ^{100}Sn in complete fusion and quasifission reactions with stable and radioactive ion beams are investigated within a dinuclear system model. The excitation functions for production of the exotic nuclei $^{100-103}$Sn and ^{112,114}Ba via xn, pxn, αxn, and ^{12,14}Cxn emission channels are predicted for future experiments.

DOI: 10.1103/PhysRevC.90.024609 PACS number(s): 25.70.Gh, 24.10.Pa, 24.60.Dr

I. INTRODUCTION

The structure and decay properties of nuclei with the $N = Z$ shell closure are challenging subjects for both experimental and theoretical studies in nuclear physics. The doubly magic nucleus ^{100}Sn [1] is of particular interest. Recent studies of decay properties of ^{100}Sn have revealed new interesting phenomena, like superallowed Gamow-Teller transition [2]. The magicity of ^{100}Sn and its neighborhood to the proton drip line is decisive for the course and the end of the astrophysical rapid-proton (rp) process [3–5]. The spontaneous emission of clusters might occur from the ground state of nuclei in this region of nuclides [6].

Several experimental studies were devoted to the production of the doubly magic nucleus ^{100}Sn in fusion-evaporation reactions. In Ref. [7], ^{100}Sn was observed as the product of the fusion-evaporation reaction ^{50}Cr + ^{58}Ni at a bombarding energy of 255 MeV. The reported production cross section of ^{100}Sn was 40 nb [7]. In Ref. [8], the smaller value of the cross section (about 3 nb) was found for the same reaction but at higher bombarding energy. The superallowed α decay of nuclei ^{109}Xe and ^{105}Te, which leads to the residual nucleus ^{101}Sn, was discovered in Ref. [9]. In Ref. [3] the superallowed α-decay chain ^{108}Xe$\rightarrow$ ^{104}Te$\rightarrow$ ^{100}Sn was proposed for producing ^{100}Sn in the ^{54}Fe(^{58}Ni,4n)^{108}Xe reaction. This method gives an alternative possibility for the production of ^{100}Sn in fusion-evaporation reactions.

One can produce ^{100}Sn in the complete fusion and quasifission reactions via the cluster emission channels. The authors of Ref. [10] studied this possibility by measuring the production cross sections of very neutron-deficient isotopes of nuclei near ^{100}Sn in the reactions ^{58}Ni + ^{50}Cr and ^{58}Ni + ^{58}Ni. In these reactions both the evaporation and the cluster emission channels lead to similar production cross sections of exotic nuclei near ^{100}Sn. Because the probability of cluster emission increases with decreasing N/Z ratio of the compound nucleus (CN) [11], the cluster emission channels might become more important in the reactions with neutron-deficient radioactive ion beams. For instance, to produce ^{100}Sn in the ^{12,14}C emission channels, one can employ the reactions leading to the CN ^{112}Ba or ^{114}Ba.

In the present work, the production excitation functions of ^{100}Sn in xn, pxn, αxn, and ^{12}Cxn channels in the fusion and quasifission reactions are predicted. Our calculations are based on the dinuclear system (DNS) model [11–14]. The DNS model [15] describes an evolution of the charge and mass asymmetry degrees of freedom [16], which are defined here by the charge and mass (neutron) numbers Z_1 and A_1 (N_1) of light nucleus of the DNS, and relative distance R coordinate. According to the model, there are nucleon drift and nucleon diffusion between the DNS nuclei, which lead to the formation of excited CN and DNS configurations (DNS with different Z_1 and A_1) with probabilities depending on the potential energy surface and temperature of the system. The main ingredient of our description is the sophisticated potential energy depending on the charge (mass) asymmetry and angular momentum. The decay of excited CN and DNS configurations can be described in a unique way, giving us an opportunity to calculate the production cross sections for residual nuclei in both light particle and heavy cluster emission channels. Thus, both light particle evaporation and complex fragment emissions are treated in the same way and the cluster emission is described under the assumption that the clusters are produced by the collective motion of the nuclear system in the charge asymmetry coordinate, with further thermal escape over the Coulomb barrier. The DNS model was successfully applied for the description of charge and mass distributions of products of the fusion and quasifission reactions. The model was able to reproduce the absolute cross sections for individual isotopes within a factor of 2–3 in the considered reactions so far [11–13].

The model is briefly described in Sec. II. The results of calculations for the reactions ^{56,58}Ni + ^{46}Ti, ^{75}Rb + ^{28}Si, ^{72}Kr + ^{40}Ca, ^{56,58}Ni + ^{50}Cr, and ^{56,58}Ni + ^{58}Ni are presented in Sec. III. The conclusions are given in Sec. IV.

II. MODEL

The cross section of the residual nucleus with certain mass number A and charge number Z is given as

$$\sigma_{Z,A}(E_{\mathrm{c.m.}}) = \sum_{J=0}^{J_{\max}} \sigma_{Z,A}(E_{\mathrm{c.m.}}, J) = \sum_{J=0}^{J_{\max}} \sigma_{\mathrm{cap}}(E_{\mathrm{c.m.}}, J) \times W^{\mathrm{sur}}_{Z,A}(E_{\mathrm{c.m.}}, J), \quad (1)$$

where $\sigma_{\rm cap}$ is the partial capture cross section which defines the transition of the colliding nuclei over the Coulomb barrier and the formation of the initial DNS when the kinetic energy $E_{\rm c.m.}$ and angular momentum J of the relative motion are transformed into the excitation energy and angular momentum of the DNS. The probability for the production of certain residual nuclei (Z,A) from the excited entrance channel DNS in a distinct decay channel is described by $W^{\rm sur}_{Z,A}(E_{\rm c.m.},J)$. To calculate $W^{\rm sur}_{Z,A}(E_{\rm c.m.},J)$, one has to find the formation-emission probability $W_{Z_1,A_1}(E_{\rm c.m.},J)$ of a certain light particle or cluster (Z_1,A_1) from the excited system. Here, we consider the decay of the excited nuclear system as a sequential light particle ($Z_1 < 2$) evaporation, which includes neutrons, protons, deuterons, and tritons, and complex clusters ($Z_1 \geqslant 2$).

The DNS formation is described by the partial capture cross section $\sigma_{\rm cap}(E_{\rm c.m.},J)$:

$$\sigma_{\rm cap}(E_{\rm c.m.},J) = \pi\lambda\!\!\!^{-2}(2J+1)P_{\rm cap}(E_{\rm c.m.},J), \qquad (2)$$

where $\lambda\!\!\!^{-2} = \hbar^2/(2\mu E_{\rm c.m.})$ is the reduced de Broglie wavelength and μ the reduced mass. The transition probability is calculated with the Hill-Wheeler formula: $P_{\rm cap}(E_{\rm c.m.},J) = (1+\exp\{2\pi[V(R_b,J)-E_{\rm c.m.}]/\hbar\omega(J)\})^{-1}$, where the effective nucleus-nucleus potential V is approximated near the Coulomb barrier at $R = R_b$ by the inverted harmonic-oscillator potential with the barrier height $V(R_b,J)$ and the frequency $\omega(J)$ [11]. The maximum value of the angular momentum, $J_{\rm max}$, is limited either by the kinematic angular momentum $J^{\rm kin}_{\rm max} = \{2\mu[E_{\rm c.m.}-V(R_b,0)]\}^{1/2}R_b$ or by the critical angular momentum $J_{\rm cr}$ depending on which one is smaller: $J_{\rm max} = \min\{J^{\rm kin}_{\rm max}, J_{\rm cr}\}$.

After the system is captured in a pocket of the nucleus-nucleus potential at $R = R_m$, the relative kinetic energy is transferred into potential and excitation energy. The DNS develops in time by diffusion in the mass-asymmetry coordinate η. Then, a statistical equilibrium is reached in the mass-asymmetry coordinate so that the formation probability P_{Z_1,A_1} of each DNS or CN configuration depends on the potential energy

$$U(R_m,Z,A,J) = B_1 + B_2 + V(R_m,Z,A,J) - \left[B_{12} + E^{\rm rot}_{12}(J)\right], \qquad (3)$$

calculated with respect to the potential energy $B_{12} + E^{\rm rot}_{12}(J)$ (here, B_{12} is the mass excess of the CN and the rotational energy $E^{\rm rot}_{12}(J)$ of the CN) of the rotational CN, where R_m is the location of the minimum of the pocket in the nucleus-nucleus interaction potential V and B_1 and B_2 are the mass excesses of fragments in their ground states. After the complete fusion, the excited CN decays by various channels including the formation of certain DNSs and their decay. In addition to the contributions from the CN decay, the binary decay component is related to the quasifission mechanism (without stage of the CN formation). The competition between the complete fusion and quasifission depends on the value of the maximum angular momentum deposited in the system. The quasifission and CN decays are hardly distinguished in the experiments because in both cases two fragments are produced by the decay of the DNS formed during the diffusion process in the mass (charge) asymmetry coordinate with and without stage of the CN formation.

The probability of the CN or DNS formation is calculated statistically by using the stationary solution of the master equation with respect to the charge and mass asymmetries and depends on the potential energy of the CN or DNS configurations (3) and on the thermodynamical temperature. The probability of the DNS decay in the R coordinate is calculated by using the transition state method. This probability depends on the difference between the potential energies of the DNS configurations at the touching distance and at the barrier position. The emission probability $W_{Z_1,A_1}(E_{\rm c.m.},J)$ of a light particle or cluster (Z_1,A_1) is calculated as the product of the CN or DNS formation probability and the CN or DNS decay probability:

$$W_{Z_1,A_1}(E_{\rm c.m.},J) = \frac{P_{Z_1,A_1}P^R_{Z_1,A_1}}{\sum_{Z'_1,A'_1}P_{Z'_1,A'_1}P^R_{Z'_1,A'_1}}, \qquad (4)$$

where the indices Z'_1 and A'_1 go over all possible channels from the neutron evaporation to the symmetric splitting. In the equilibrium limit of the master equation in the charge and mass asymmetries (see Ref. [11] for details), the probability P_{Z_1,A_1} is given by

$$P_{Z_1,A_1}(E_{\rm c.m.},J) \sim \exp[-U(R_m,Z_1,A_1,J)/T_{\rm max}(J)]. \qquad (5)$$

Here, n, p, d, and t evaporation channels are taken into consideration with $U(R_m,Z_1,A_1,J) = 0$. The quasifission barrier $B^{\rm qf}_R$, calculated as the difference between the bottom of the inner pocket and the top of the external barrier, prevents the decay of the DNS in R degrees of freedom with the factor $P^R_{Z_1,A_1}$ given as

$$P^R_{Z_1,A_1}(E_{\rm c.m.},J) \sim \exp\left[-B^{\rm qf}_R(Z_1,A_1,J)/T_{Z_1,A_1}(J)\right]. \qquad (6)$$

In Eqs. (5) and (6), $T_{\rm max}(J) = \max\{T_{Z_1,A_1}(J)\}$, where $T_{Z_1,A_1}(J)$ are the temperatures of the CN and all possible DNSs. For the emission of particles with $Z_1 < 2$, $T_{Z_1,A_1}(J) = T_{\rm CN}(J)$ is the temperature of the CN and $B^{\rm qf}_R(Z_1,A_1,J)$ is equal to the particle binding energy plus the value of the corresponding Coulomb barrier at $Z_1 \neq 0$. The Fermi-gas model is employed to compute the temperature [11–14].

The neutron-deficient isotopes of nuclei are usually produced in very weak decay channels and their absolute production cross sections are very sensitive to the excitation energy which is available for light particle or cluster emission. After emission of a light particle or cluster, the excitation energy of the residual nucleus depends on the emission barrier $B^{\rm qf}_R(Z_1,A_1,J)$ and the kinetic energy of the emitted particle or cluster. In Ref. [11], the kinetic energies of emitted particles were assumed to be $2T_{Z,A}(J)$ on average. Here, we modified our calculations by taking into account the kinetic energy distributions of emitted light particles (n, p, d, and t) and clusters (^{3}He, ^{4}He, ^{12,14}C, ...) as

$$P(\epsilon,J) = \epsilon\exp[-\epsilon/T_{Z,A}(J)], \qquad (7)$$

where ϵ is the kinetic energy of a light particle or cluster in the center-of-mass system. The actual value of ϵ in each decay

TABLE I. The comparison of the calculated production cross sections $\sigma_{Z,A}$ for the indicated residual nuclei (ER) with the experimental ones $\sigma_{Z,A}^{\rm expt}$. The weights (in %) of the main production channels are derived from our calculations. The experimental data are from Refs. [3,7,10].

Reactions	$E_{\rm lab}$ (MeV)	$E^*_{\rm CN}$ (MeV)	$J_{\rm max}$	ER	$\sigma_{Z,A}^{\rm expt}$ (μb)	$\sigma_{Z,A}$ (μb)	Production channels (weights in %)
^{58}Ni + ^{50}Cr	319	102	75	^{100}In	2.6	5.6	$\alpha p3n$
^{58}Ni + ^{58}Ni	325	96	78	^{100}In	0.8	3.1	^{12}C$p3n$ (80%), 3$\alpha p3n$ (20%)
^{58}Ni + ^{58}Ni	348	107	78	^{100}In	1.7	5.2	^{12}C$p3n$ (60%), 3$\alpha p3n$ (40%)
^{58}Ni + ^{58}Ni	371	119	78	^{100}In	1.7	3.2	^{12}C$p3n$ (40%), 3$\alpha p3n$ (60%)
^{58}Ni + ^{58}Ni	394	131	78	^{100}In	1.6	0.86	^{12}C$p3n$ (10%), 3$\alpha p3n$ (90%)
^{58}Ni + ^{50}Cr	249	70	64	^{101}Sn	$(1.6 \pm 0.4) \times 10^{-2}$	8.2×10^{-2}	$\alpha 3n$
^{58}Ni + ^{58}Ni	325	96	78	^{101}Sn	$(0.9 \pm 0.4) \times 10^{-2}$	5.0×10^{-2}	^{12}C3n (70%), 3$\alpha 3n$ (30%)
^{58}Ni + ^{58}Ni	348	107	78	^{101}Sn	$(1.3 \pm 0.3) \times 10^{-2}$	4.2×10^{-2}	^{12}C3n (50%), 3$\alpha 3n$ (50%)
^{58}Ni + ^{58}Ni	371	119	78	^{101}Sn	$(2.8 \pm 1.0) \times 10^{-2}$	3.6×10^{-2}	^{12}C3n (35%), 3$\alpha 3n$ (65%)
^{58}Ni + ^{58}Ni	394	131	78	^{101}Sn	$(0.7 \pm 0.4) \times 10^{-2}$	0.6×10^{-2}	^{12}C3n (5%), 3$\alpha 3n$ (95%)
^{58}Ni + ^{54}Fe	200	40	27	^{110}Xe	1.0 ± 0.2	0.7	2n
^{58}Ni + ^{54}Fe	215	47	40	^{109}Xe	$(1.0 \pm 0.2) \times 10^{-2}$	5.8×10^{-2}	3n
^{50}Cr + ^{58}Ni	255	92	75	^{100}In	1.0	0.8	$\alpha p3n$
^{50}Cr + ^{58}Ni	255	92	75	^{100}Sn	4.0×10^{-2}	1.0×10^{-2}	$\alpha 4n$

event is chosen via the Monte Carlo method. This modification affects the cross sections in very weak decay channels and has almost no influence on the major decay channels.

In the calculations, we use formulas (1) and (4) to treat the sequential statistical decay (the evaporation of light particles and/or the binary decay) of the hot CN. The generation of a whole cascade of decay channels is performed via the Monte Carlo method. We continue to trace the decay processes until all fragments become cold (the excitation energy of a fragment is smaller than its neutron emission threshold). The number n of the generated events in the Monte Carlo technique was chosen according to the smallest decay probability, which is $\sim 1/n$. The number of iterations, $n > 10^4$, is large enough to obtain the calculated results with quite a high accuracy.

III. RESULTS AND DISCUSSIONS

A. Comparison with experimental data

To test the method suggested, we treated the production cross sections of exotic nuclei in very weak decay channels. In Table I and Fig. 1, the calculated cross sections are in a good agreement with the experimental data for the reactions ^{58}Ni + ^{50}Cr, ^{58}Ni + ^{58}Ni, and ^{58}Ni + ^{54}Fe [3,7,10]. Note that our model reproduces the experimental data without adjusting the separation energies of light particles and clusters. So, the model can be employed for the predictions of excitation functions of exotic nuclei in the fusion and quasifission reactions.

In Table I, some residual nuclei result from both light particle and light cluster emission channels. The competition between different production channels depends on the

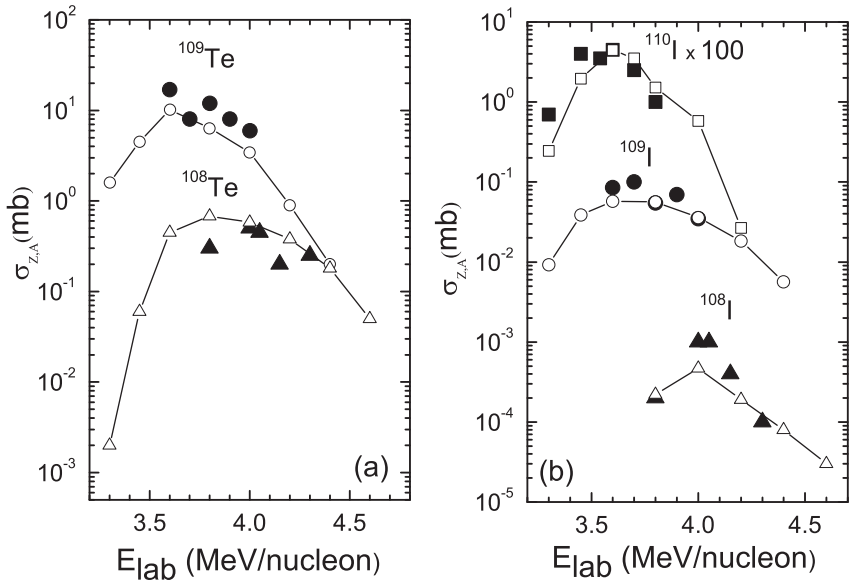

FIG. 1. The comparison of experimental (solid symbols) and calculated (open symbols connected by line) excitation functions for production of indicated isotopes of (a) Te and (b) I in the ^{58}Ni + ^{54}Fe reaction. The experimental data are from Ref. [3].

available excitation energy and angular momentum. For the ^{58}Ni + ^{58}Ni reaction, with increasing excitation energy the ^{12}C emission channel gives a smaller contribution to the formation of residual nuclei ^{100}In and ^{101}Sn because after the emission of ^{12}C more excitation energy is left in the daughter nucleus and further emission of light particles results a residual nucleus with lower Z and/or A. For example, 3α emission takes away almost twofold more excitation energy than the ^{12}C emission. Therefore, at high excitation energies the main production channel of residual nuclei ^{100}In and ^{101}Sn is related to the 3α emission channel. Thus, the excitation energy and formation channels determine the angular momentum range for the formation of certain residual nuclei. At angular momenta $J > 60$, the quasifission process from nearly symmetric configurations dominates and the evaporation residue cross sections strongly decrease. Because the CN formed in these reactions are very neutron deficient, the neutron evaporation process is strongly suppressed.

Comparing cross sections in Table I to those from Ref. [17], one can conclude that the agreement between calculated and experimental cross sections is considerably improved when the kinetic energy distributions (7) of emitted light particles and light clusters are taken into consideration instead of their average kinetic energies. Because of this modification, the production cross sections are more affected in the weak decay channels. For example, in the ^{50}Cr + ^{58}Ni reaction at a bombarding energy of 255 MeV, the production cross section in the $\alpha 4n$ channel increases by a factor of 4 because this channel is realized in broader angular momentum range at the available excitation energy.

B. Production of ^{100}Sn in xn decay channels

The difficulties of the production of ^{100}Sn in fusion-evaporation reactions are mainly related to the drastically small probability of neutron emission from neutron-deficient CN. In more symmetric reactions Zn + Ca, Ti + Ni, and Cr + Fe with stable beams, one can produce the most neutron-deficient CN, ^{104}Sn. By employing reactions with radioactive beams, one can form even lighter isotopes of Sn.

For the ^{58}Ni + ^{46}Ti reaction, the excitation functions for the production of $^{100-103}$Sn are given in Fig. 2. Because 3n and 4n decay channels can be realized in broader angular momentum and excitation energy ranges than 1n and 2n decay channels, the excitation functions for the production of ^{100,101}Sn are broader than those for the production of ^{102,103}Sn. Also noticeable is that the maximum of the excitation function for even nucleus ^{102}Sn is one order of magnitude larger than the corresponding maximum for odd nucleus ^{103}Sn, while the maximum production cross section for ^{101}Sn is six times larger than the corresponding value for ^{100}Sn. In the former case, such a difference in the cross sections is mainly related to the expenses of excitation energy and angular momentum at which 1n and 2n decay channels can be realized. In the latter case, the reasons are the small binding energy of the proton and the large binding energy of the neutron which prevent the formation of the lighter isotopes of Sn. The maximum value of the production cross section for ^{100}Sn in this reaction at 4.0–4.2 MeV/nucleon is about 30 nb.

The calculated excitation functions for the production of ^{100,101}Sn in the ^{56}Ni + ^{46}Ti reaction are also shown in Fig. 2. In this case, the maximum value of the production cross section for ^{100}Sn is about 500 nb. One can see that the ratio of production cross sections for ^{100}Sn in the reactions ^{56}Ni + ^{46}Ti and ^{58}Ni + ^{46}Ti is about 20. The actual yield of ^{100}Sn depends on the intensities of corresponding stable and radioactive beams. One can see that the production cross section for ^{100}Sn is larger than for ^{101}Sn. This can be explained again as a consequence of expenses of excitation energy and angular momentum at which 1n and 2n decay channels can be realized. For example, in the ^{56}Ni(3.4 MeV/nucleon) + ^{46}Ti reaction, the excitation energies of the CN ^{102}Sn at the angular momenta $J = 0$ and $J = J_{max} = 28$ are 52 and 38 MeV, respectively, which are quite large for the evaporation of only one neutron. With increasing bombarding energy, J_{max} increases and the available excitation energy for evaporation of particles at $J = J_{max}$ decreases. In the ^{56}Ni(4.0 MeV/nucleon) + ^{46}Ti

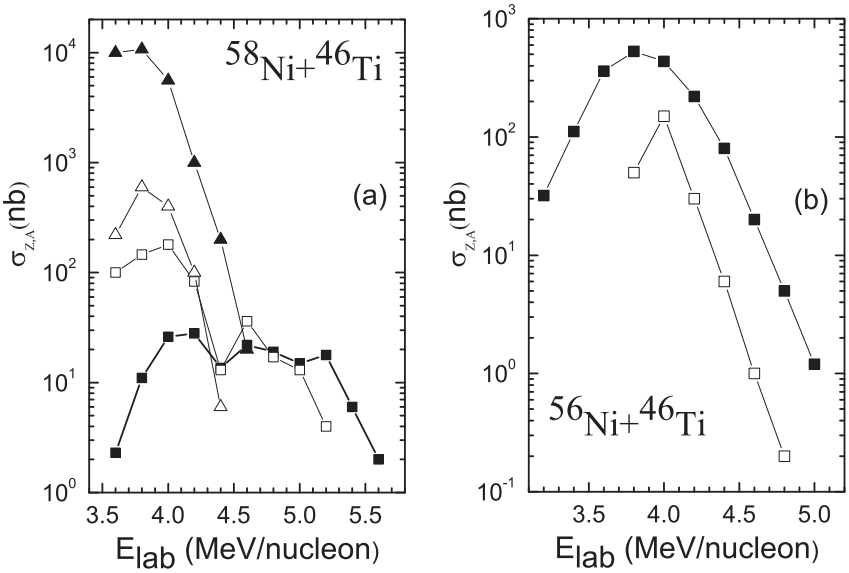

FIG. 2. The calculated excitation functions for the production of ^{100}Sn (■), ^{101}Sn (□), ^{102}Sn (▲), and ^{103}Sn (△) in xn-decay channels of the reactions (a) ^{58}Ni + ^{46}Ti and (b) ^{56}Ni + ^{46}Ti.

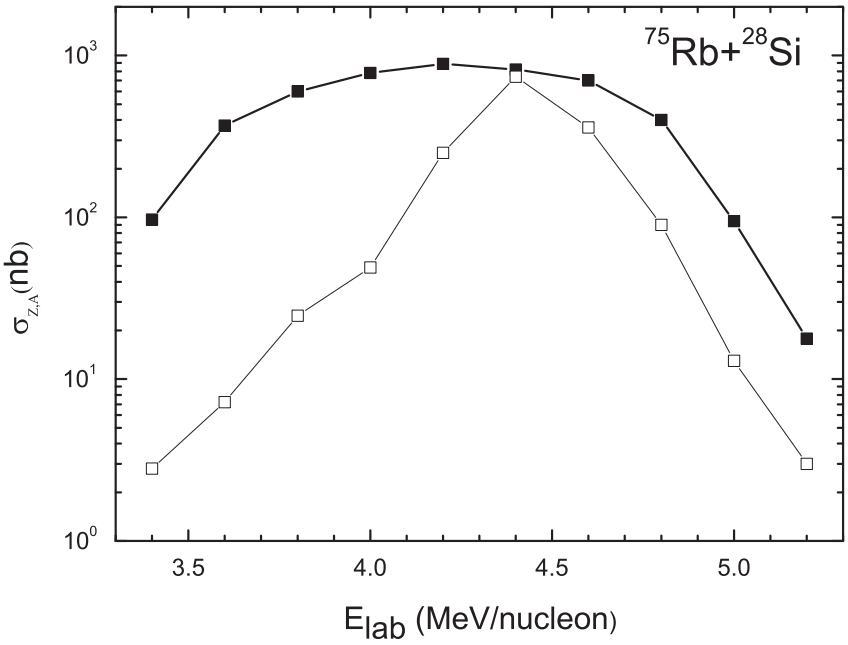

FIG. 3. The calculated excitation functions for the production of ^{100}Sn (■) and ^{101}Sn (□) in pxn-decay channels of the ^{75}Rb + ^{28}Si reaction.

reaction at $J_{max} = 52$, the excitation energy of the CN is equal to 20 MeV, which makes possible the evaporation of only one neutron at angular momenta close to J_{max}.

For the reactions ^{64,62}Zn + ^{40}Ca, ^{54,52}Fe + ^{50}Cr, and ^{44}Ti + ^{58}Ni, the calculated production cross sections for ^{100}Sn in the corresponding decay channels are similar to those for the reactions ^{58,56}Ni + ^{46}Ti.

C. Production of ^{100}Sn in pxn decay channels

As found, in the fusion reactions with stable beams, the absolute production cross sections of the ^{100}Sn nucleus via the optimal $p8n$ decay channel are at the level of picobarns. That is why we present only the cross sections for the reactions with radioactive beams. As an example, the excitation functions for production of ^{100,101}Sn in the ^{75}Rb + ^{28}Si reaction are shown in Fig. 3. The maximum production cross section of ^{100}Sn in this reaction via the $p2n$ decay channel is 890 nb. Because of the high probability of proton evaporation from the excited neutron-deficient Sb isotopes, the behavior of excitation functions and maximum production cross section for ^{100}Sn in pxn decay channels are similar to those in the xn decay channels. One can also see that the excitation functions for production of ^{100}Sn are broader than those for production of ^{101}Sn. Similar results can be obtained in other possible reactions leading to the same CN.

D. Production of ^{100}Sn in αxn decay channels

Various reactions with stable and radioactive beams, for example, ^{54}Fe + ^{54}Fe or ^{56,58}Ni + ^{50}Cr, can be employed for the production of ^{100}Sn via αxn channels. In the fusion

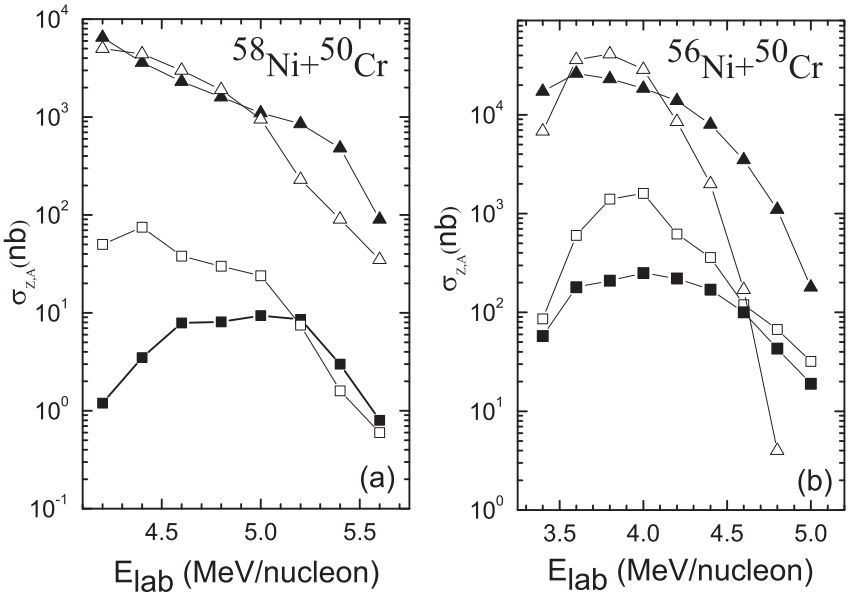

FIG. 4. The calculated excitation functions for the production of ^{100}Sn (■), ^{101}Sn (□), ^{102}Sn (▲), and ^{103}Sn (△) in αxn-decay channels of the reactions (a) ^{58}Ni + ^{50}Cr and (b) ^{56}Ni + ^{50}Cr.

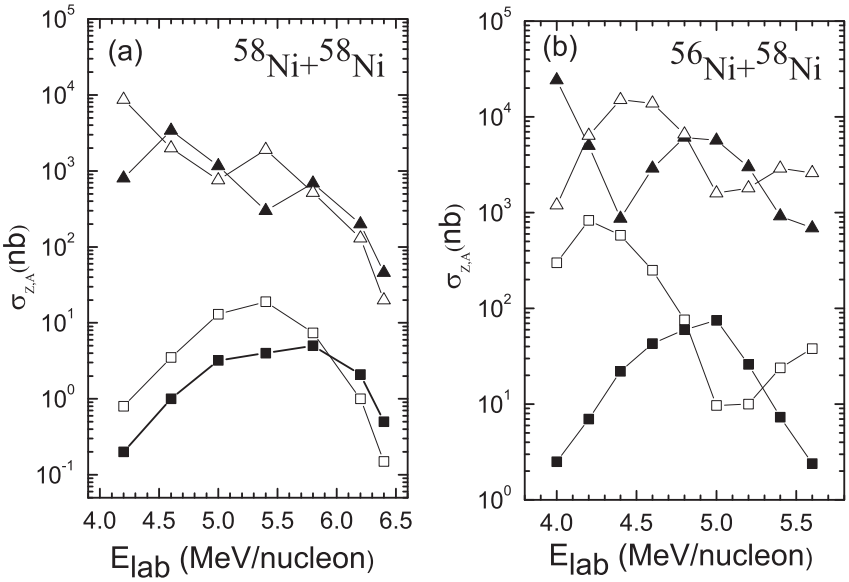

FIG. 5. The calculated excitation functions for the production of ^{100}Sn (■), ^{101}Sn (□), ^{102}Sn (▲), and ^{103}Sn (△) in cluster emission channels of the reactions (a) ^{58}Ni + ^{58}Ni and (b) ^{56}Ni + ^{58}Ni. See the text for details.

reactions ^{54}Fe + ^{54}Fe and ^{58}Ni + ^{50}Cr with stable beams and in the ^{56}Ni + ^{50}Cr reaction with a radioactive beam, the optimal production channels are $\alpha 4n$ and $\alpha 2n$, respectively (Fig. 4). The calculated maximum production cross sections for ^{100}Sn in the reactions ^{58}Ni + ^{50}Cr and ^{56}Ni + ^{50}Cr are 10 and 250 nb, respectively. For a comparison, the experimental production cross section of ^{100}Sn in the ^{58}Ni + ^{50}Cr reaction at energy 5.1 MeV/nucleon is 40 nb [7]. One should mention that the residual nucleus ^{104}Te may lead also to the ^{100}Sn via superallowed α decay. Such a contribution to the production cross section of ^{100}Sn is not taken into consideration in Fig. 4.

E. Production of ^{100}Sn in cluster decay channels

The production of ^{100}Sn in the fusion and quasifission reactions via cluster decay channels is mainly connected with the emission of ^{12,14}C due to the largest emission probability of carbon among heavy clusters. Hence, we consider the reactions ^{56,58}Ni + ^{58}Ni and ^{72}Kr + ^{40}Ca leading to the CN of barium. In Fig. 5, we present the calculated excitation functions for the production of $^{100-103}$Sn in the reactions ^{56,58}Ni + ^{58}Ni. It is seen that the excitation function becomes wider with an increasing amount of evaporated particles. The excitation functions may have several maxima which correspond to different decay channels. The cluster decay channels are realized at low bombarding energies. With increasing bombarding energy, the light particle evaporation channels become dominant. For the reactions ^{58}Ni + ^{58}Ni at 5.6–5.8 MeV/nucleon [^{56}Ni + ^{58}Ni at 4.8–5.0 MeV/nucleon], the main decay channels leading to the production of ^{100}Sn are ^{12}C4n (40%) and ^{14}C2n (60%) [^{12}C2n (20%) and ^{14}C (80%)]. For the reactions ^{58}Ni + ^{58}Ni and

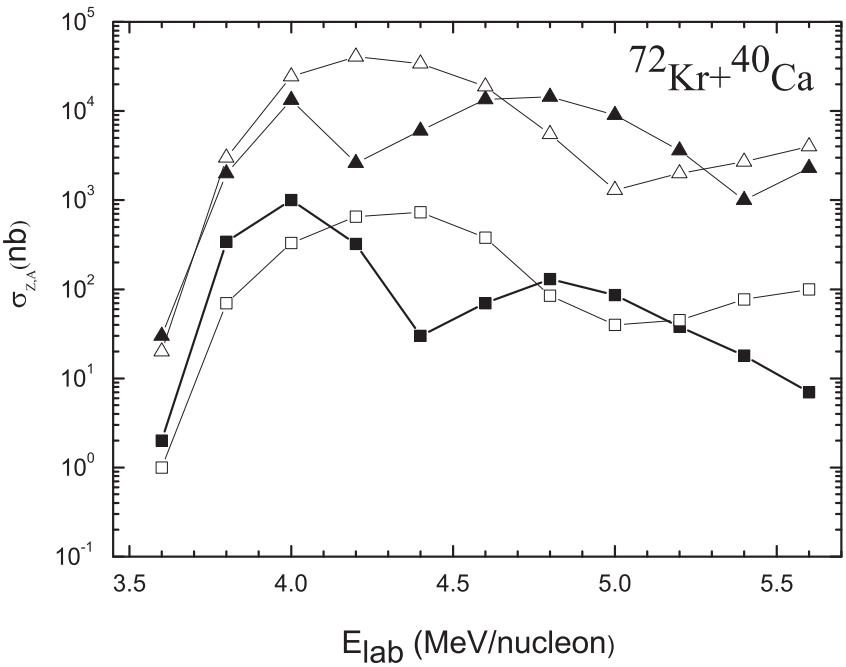

FIG. 6. The same as in Fig. 5, but for the ^{72}Kr + ^{40}Ca reaction.

^{56}Ni + ^{58}Ni, the maximum production cross sections are about 5 and 75 nb, respectively.

Note that the production of isotopes of barium, ^{114}Ba and ^{112}Ba, in the reactions ^{58,56}Ni + ^{58}Ni could be also interesting. These isotopes are good candidates for the study of cluster radioactivity (^{12,14}C). For the reactions ^{58,56}Ni + ^{58}Ni, the maximum production cross sections for ^{114}Ba and ^{112}Ba are 25 and 16 nb, respectively.

For the ^{72}Kr + ^{40}Ca reaction with the radioactive beam, we present the excitation functions for the production of exotic nuclei $^{100-103}$Sn (Fig. 6). One can observe that the excitation function for ^{100}Sn has two maxima at energies 4.0 and 4.8 MeV/nucleon which correspond to the decay channels ^{12}C and 3α, respectively. The maximum production cross sections corresponding to the emission channels ^{12}C and 3α are 1 μb and 130 nb, respectively.

IV. CONCLUSION

This work provides the DNS model systematics of the production cross sections of the doubly magic nucleus ^{100}Sn in the fusion and quasifission reactions via all possible optimal decay channels including light particle evaporation and light cluster emission channels. The results of calculations show that the maximum production cross sections of ^{100}Sn are about 30 nb in the ^{58}Ni + ^{46}Ti reaction with a stable beam and about 1 μb in the reactions with radioactive beams. By taking into consideration the beam intensities and optimal production cross sections, we found that the best candidate for the production of ^{100}Sn among reactions with radioactive ion beams is the ^{56}Ni + ^{46}Ti reaction via the $2n$ emission channel. The production cross sections of the doubly magic nucleus ^{100}Sn via light particle evaporation and cluster emission channels are comparable. The production cross sections for the nuclei $^{101-103}$Sn via xn, pxn, αxn, and cluster decay channels were predicted as well.

ACKNOWLEDGMENT

This work was partially supported by RFBR and the IN2P3-JINR cooperation program.

[1] T. Faestermann *et al.*, Prog. Part. Nucl. Phys. **69**, 85 (2013).
[2] C. B. Hinke *et al.*, Nature (London) **486**, 341 (2012).
[3] A. Korgul *et al.*, Phys. Rev. C **77**, 034301 (2008).
[4] H. Schatz *et al.*, Phys. Rev. Lett. **86**, 3471 (2001).
[5] C. Mazzocchi *et al.*, Phys. Rev. Lett. **98**, 212501 (2007).
[6] S. N. Kuklin, G. G. Adamian, and N. V. Antonenko, Phys. Rev. C **71**, 014301 (2005).
[7] M. Chartier *et al.*, Phys. Rev. Lett. **77**, 2400 (1996).
[8] M. Karny *et al.*, Eur. Phys. J. A **25**, 135 (2005).
[9] S. N. Liddick *et al.*, Phys. Rev. Lett. **97**, 082501 (2006).
[10] M. La Commara *et al.*, Nucl. Phys. A **669**, 43 (2000).
[11] Sh. A. Kalandarov, G. G. Adamian, N. V. Antonenko, and W. Scheid, Phys. Rev. C **82**, 044603 (2010); S. A. Kalandarov, G. G. Adamian, N. V. Antonenko, W. Scheid, and J. P. Wieleczko, *ibid.* **84**, 064601 (2011).
[12] S. A. Kalandarov, G. G. Adamian, N. V. Antonenko, and W. Scheid, Phys. Rev. C **83**, 054611 (2011).
[13] Sh. A. Kalandarov *et al.*, Phys. Rev. C **84**, 054607 (2011).
[14] G. Ademard *et al.*, Phys. Rev. C **83**, 054619 (2011).
[15] V. V. Volkov, Izv. Akad. Nauk SSSR Ser. Fiz. **50**, 1879 (1986); G. G. Adamian, A. K. Nasirov, N. V. Antonenko, and R. V. Jolos, Phys. Part. Nucl. **25**, 583 (1994); G. G. Adamian, N. V. Antonenko, and W. Scheid, Nucl. Phys. A **618**, 176 (1997); G. G. Adamian, N. V. Antonenko, W. Scheid, and V. V. Volkov, *ibid.* **627**, 361 (1997); **633**, 409 (1998); G. G. Adamian, N. V. Antonenko, and W. Scheid, Phys. Rev. C **68**, 034601 (2003).
[16] W.-U. Schröder and J. R. Huizenga, in *Treatise on Heavy-Ion Science*, edited by D. A. Bromley, Vol. 2 (Plenum Press, New York, 1984), p. 115; V. V. Volkov, in *Treatise on Heavy-Ion Science*, edited , Vol. 8 (Plenum Press, New York, 1989), p. 101.
[17] Sh. A. Kalandarov *et al.*, EPJ Web Conf. **17**, 10004 (2011).